Available online at www.sciencedirect.com
SCIENCE DIRECT
Conference of Global Chinese Scholars on Hydrodynamics

LARGE-EDDY SIMULATION FOR URBAN MICRO-METEOROLOGY

Zhengtong XIE, Ian P. CASTRO
School of Engineering Sciences, University of Southampton, Southampton SO17 1BJ, UK
E-mail: z.xie@soton.ac.uk, i.castro@soton.ac.uk

ABSTRACT: Validation of large-eddy simulation (LES) computations of flows over an array of cubes with imposed periodic inflow-outflow condition is described. Then, a method of generation of appropriate inflow data for such flows is proposed and the results are compared with those using periodic boundary conditions in the streamwise direction and wind tunnel measurements [3]. Finally, some results obtained using the inflow method for an oscillatory through-flow combined with a steady current are discussed.

KEYWORDS: inlet condition, oscillatory flow, street scale, weather scale, urban environment.

1. Introduction

Heat, mass and momentum transfer in atmospheric boundary layers (ABL) within and above an urban area are of fundamental and practical importance. In particular, understanding of the mechanisms by which the urban boundary layer, the rural boundary layer, the city scale flow [2], the regional weather and the general circulation of the atmosphere, are coupled aerodynamically and thermodynamically is very important but still in its infancy. For instance, the temperature in cities has been found to be up to ten degrees higher than the surrounding rural areas, and to cause large increases in rainfall amounts downwind; however, there are situations in which urban aerosol suppresses precipitation [6]. The grid square is no less than about one kilometre on a side in most general circulation models (GCM) or operational regional weather models. To investigate the micro-meteorology in an urban area down to the resolution one meter, computational fluid dynamics (CFD) must inevitably applied. Nevertheless, the urban area, which is composed of buildings, streets, parks, etc. is a considerable challenge to CFD.

A number of major observations of flow and dispersion in urban areas have been completed recently and more are planned [2]. Large-eddy simulation (LES) is a promising tool for computing unsteady 3-D flows at high Reynolds number or with complex geometry [20]. Flow over groups of cubes mounted on a wall provides an excellent test case for validation of LES. The groups of cubes represent either simple buildings or roughness elements. Furthermore, understanding of such flows is also directly beneficial to the understanding of building aerodynamics, urban meteorology and atmospheric boundary layer meteorology [2, 19, 3, 5, 8, 11]. Nevertheless, further studies applying LES to 3-D flow over obstacle arrays are still needed [11].

In Section 2, validated simulations of flow over wall- mounted uniform cubes using large-eddy simulation with periodic boundary conditions in the streamwise and lateral directions are presented, by comparing with direct numerical simulation, RANS modelling and wind tunnel experiment. We have also simulated flow over 64 random-height obstacles, which is more realistic for urban environments. In Section 3, a quasi-steady inlet condition is developed and implemented with carefully designed artificially imposed turbulence fluctuations. Our ambitious, longer-term objective is to develop tools for implementing unsteady spatial boundary conditions derived from the output of much larger-scale computations, e.g. the UK Met Office's Unified Model, with the LES code for computing the street-scale flow. As a start and a validation, a combined oscillatory through-flow and steady current over a group of cube arrays imposing quasi-steady inlet conditions has been simulated and results compared with those obtained by imposing a combined oscillatory and steady pressure gradient with periodic boundary conditions.

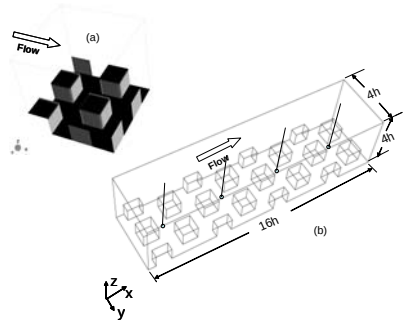

Fig. 1 Schematic view of the domains used for: (a) periodic boundary condition in streamwise direction, (b) inflow boundary condition. The four vertical lines indicate the data sampling locations, which are labelled from left to right as "behind row 1", "behind row 3", "behind row 5" and "behind row 7".

2. Validation Sing Periodic Inflow-outflow Condition

Our main interest in this paper is on the urban environment, so we are mostly concerned with the flow within the cube-canopy and above it, up to a height at least equal to the top of roughness sublayer (the region in which the flow is spatially inhomogeneous). LES was applied to calculate the turbulent flow over four staggered wall-mounted cubes (see figure 1a). The plan area density of the cubic array was 0.25. In the streamwise and lateral directions the flow was periodic. A constant pressure gradient was imposed on every cell as the driving force. To validate the mesh resolution, coarse (LES8, 8 grids on the cube), medium (LES16, 16 grids on the cube) and fine meshes (LES32, 32 grids on the cube) were used to simulate the flow at a Reynolds number of 5000, based on the free stream velocity and the cube height. Vertical profiles of mean velocity, velocity fluctuation and shear stress at four typical locations above and within the cube-canopy are in reasonable in figure 4. The LES with medium mesh has yielded satisfactory results. In particular, note that the results of LES8 (a much coarser mesh) are also in reasonable agreement with DNS (64 grids on the cube).

In particular, we address three issues. Firstly, how large is the Reynolds number dependency? This is crucial when a wind tunnel model is used for investigation of a full scale model. By simulating the flows over staggered uniform cubes we found the Reynolds number dependency is very weak in the range Re=5×10^3 to 5×10^6, with Re based on the cube height and the free stream velocity. This is because the flows are building scale dominated and the flows within and immediately above the canopy are fully three-dimensional. Secondly, how important are the wall-layers on the building surfaces? The computation domain typically may contain tens or hundreds of buildings. For instance, the DAPPLE geometry, which is one we are currently simulating, has nearly one hundred buildings. To resolve all of the wall layers is extremely expensive at present. By using numerical experiments, we found that full resolution of the wall-layers is not important for the global turbulence statistics, nor for the mean drag of the complete surface. Finally, how much detail of the flow within the urban canopy layer is important? This highly depends on the arrangement of the blocks. The validation suggests that LES is reliably able to simulate the turbulent flow over urban-like obstacles with grids significantly coarser than required for a full DNS.

3. Generation of Inflow Dada

Klein et al. 12] developed a technique generating artificial velocity as inflow data for jet flows, which reproduces first and second order one point statistics

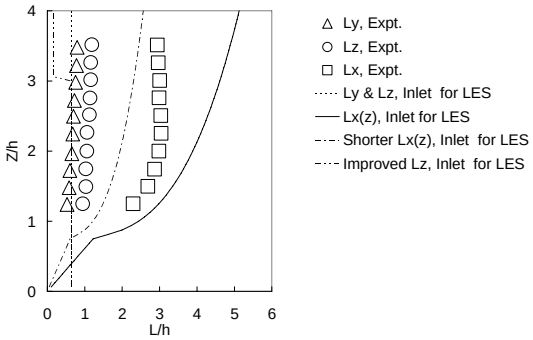

Fig. 2 Integral length scales of inflow data

as well as a locally given autocorrelation. Based on the knowledge that for homogeneous turbulence in a late stage, the autocorrelation function takes a Gaussian form, Klein *et al.* used a Gaussian function filtering the 3-D random data. In the current paper, a fully developed turbulent flow was simulated. The autocorrelation function of such flows is found to have a form closer to exponential than Gaussian [17], and given by

$$R(r,0,0) = \exp\left(-\frac{\pi r}{2L}\right), \qquad (1)$$

where L is the length scale. Hanna *et al* [8] also used an exponential formula to generate a 1-D time series of inflow data. We therefore applied an exponential function for filtering the 3-D random data. With $L = n\Delta x$, where Δx is the grid size, the autocorrelation function can be rewritten as,

$$\frac{\overline{u_m u_{m+k}}}{\overline{u_m u_m}} = R_{uu}(k\Delta x) = \exp\left(-\frac{\pi|k|}{2n}\right). \qquad (2)$$

A filter function is written as follows,

$$u_m = \sum_{j=-N}^{N} b_j r_{m+j}, \qquad (3)$$

where r_m is a series of random data with $\overline{r}_m = 0$, $\overline{r_m r_m} = 1$. The bj are the filter coefficients and N is related to the length scale of the filter. Here we take $N \geq 2n$. We can easily get the mean value $\overline{u}_m = 0$.

Because $\overline{r_m r_n} = 0$ for $m \neq n$, we also can obtain,

$$\overline{u_m u_{m+k}} = \sum_{j=-N+k}^{N} b_j b_{j-k}. \qquad (4)$$

The filter coefficients are then obtained,

$$b_k \approx \tilde{b}_k \Big/ \left(\sum_{j=-N}^{N} \tilde{b}_j^2\right)^{1/2}, \qquad (5)$$

where the denominator on the right of the equation is simply a normalizing factor to obtain $\overline{u_m u_m} = 1$, and

$$\tilde{b}_k = \exp\left(-\frac{\pi|k|}{n}\right). \quad (6)$$

Note equation 5 is only approximatively valid. Using equation 3 and 5, a series of data (1-D) with mean value $\overline{u}_m = 0$, variance $\overline{u_m u_m} = 1$ and prescribed length scale *L*, are obtained.

A 2-D filter can be obtained as,

$$b_{jk} = b_j b_k. \quad (7)$$

The above 2-D filter is applied to filter a 2-D slice of random data of dimensions [*-Ny+1:My+Ny, -Nz+1: Mz+Nz*], where *My* ×*Mz* are the dimensions of the grid in the inflow plane, $N_\alpha \geq 2n_\alpha$, α=*y, z*. A 2-D slice of data $\Psi_\alpha(t, y, z)$ with prescribed length scale $L_\alpha = n_\alpha \Delta_\alpha$ [3] is obtained. For the next time step,

$$\Psi_\alpha(t+\Delta t, y, z) = \Psi_\alpha(t, y, z)\exp\left[-\pi\Delta t/(2T)\right] + \psi(t, y, z)\sqrt{1-\left[\exp\left[-\pi\Delta t/(2T)\right]\right]^2}, \quad (8)$$

where $\psi(t, y, z)$ is obtained in the same way as $\Psi_\alpha(t, y, z)$ but filtering a new set of random data. *T* is the Lagrangian time scale, which is calculated from the measurements [3] using Taylor's hypothesis. Because $\psi(t, y, z)$ is independent of $\Psi_\alpha(t, y, z)$ and fully random in time *t*, it can be deduced from equation (8) that the variance of Ψ_α is unity. Note in equation (8) $\sqrt{1-\left[\exp\left[-\pi\Delta t/(2T)\right]\right]^2}$ ranges from *R(1.2Lx, 0, 0)* to *R(2Lx, 0, 0)* for $1/1000 \leq \pi\Delta t/(2T) \leq 1/100$, where *Lx* is the length scale in *x* direction. Overall, equation (8) is quite similar to the 3-D digital filter [12]. But note that equation (8) only calculates two 2-D slices of data, whereas Klein's method calculates *2Nx* 2-D slices of random data. Hence, the present method is much more economical, in particular when the length scale is large. Hanna *et al.* [8] used a method similar to equation 8 in generating a 1-D time series of inflow data, but without spatial correlation in vertical and lateral directions, which is a serious drawback.

Finally, the following transformation proposed by Lund *et al* [15] is performed:

$u_i = \bar{u}_i + a_{ij}\Psi_j$ with $a_{11} = (\hat{R}_{11})^{1/2}$,

$a_{21} = \hat{R}_{21}/a_{11}$, $a_{22} = (\hat{R}_{22} - (a_{21})^2)^{1/2}$,

$a_{33} = (\hat{R}_{33})^{1/2}$,

where $\hat{R}_{ij}$ is the prescribed correlation tensor, which is obtained from the wind tunnel experiment or the previous numerical simulation with periodic inlet-outlet condition. Other elements of matrix a_{ij} are all zero.

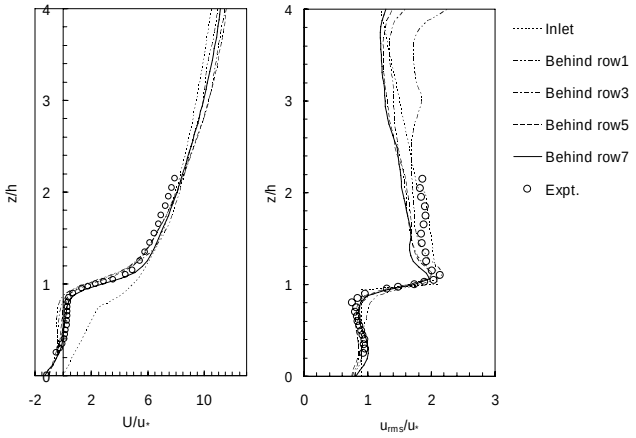

Fig. 3 Convergence to fully-developed condition

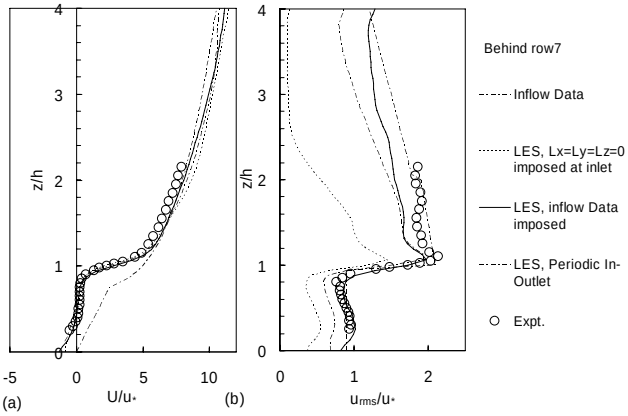

Fig. 4 Vertical profiles of time averaged streamwise velocity (a) and turbulence intensity (b)

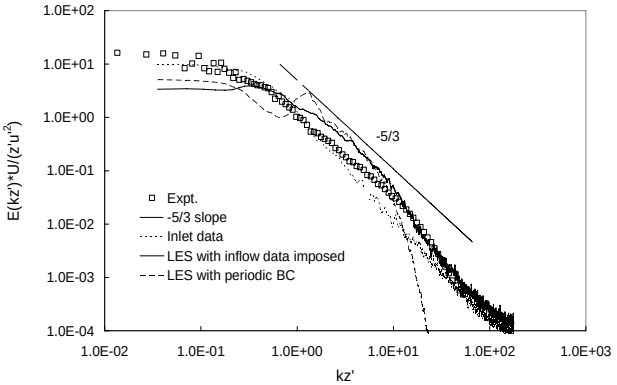

Fig. 5 Spectra of the axial turbulence component, plotted in inner-layer scaling. "LES with inflow data imposed" was sampled at z = 1.5h on row seven

We simulated flows over 8 rows of staggered cubes (4 repeated units of the periodic case in the streamwise direction, see figure 1b) imposing the synthetic inflow data and zero-gradient outflow conditions. The integral length scales are shown in figure 2. The other boundary conditions are the same

as in the periodic case. We noted that the statistics profiles very likely have reached an equilibrium state beyond the fifth row downstream (see figure 3). Figure 4 shows a comparison between the synthetic inlet case and the periodic case. The length scales for "LES, inflow data imposed" are the "Lx(z), inlet for LES", "Ly, inlet for LES" and "improved Lz, inlet for LES" in figure 2. We found that the latter, having a lower value in the vicinity of the upper free-slip plane, gave better performance. By also reducing Lx by one half ("shorter Lx(z), inlet for LES" in figure 2), the LES would also not produce such a large discrepancy in the upper part of the flow in the subsequently studied oscillatory inflow cases (see Section 4). Note in figure 4 that fully random fluctuations ($Lx=Ly=Lz=0$) with the same turbulence intensities at the inlet decayed quickly downstream, in particular in the region above the canopy.

Figure 5 shows typical spectra, plotted in inner-layer scaling. Note that $k=2\pi f/U$ is the wavenumber and $z'=z-d$, where d=0.013m is the zero-plane displacement [3]. The data were sampled at z = 1.5h (for the case "LES with inflow data imposed", the data were sampled at z=1.5h on row seven). A wide (e.g. more than one decade) inertial sub-range with slope -5/3 was found on the spectrum obtained from measurements at a low Reynolds number of approximately 5000 [16, 3], which is usually found away from a smooth solid wall only at much higher Reynolds number. This again confirms that turbulence generated by urban-like obstacles (with sharp edges) is large-scale dominated.

In figure 5, the "LES with periodic BC" resolved a narrow inertial sub-range of the spectrum. There is a rapid drop beyond about $kz' = 10$ for the "LES with periodic BC", which is certainly due to the relatively low spatial resolution. The spectrum of "inlet data" is in good agreement with the measurements, which again suggests that the method is satisfactory. Note that a rapid drop at high frequencies is not present in the spectrum of "LES with inflow data imposed". This must be because the inlet spectrum is "fully" re-solved in time and the axial fetch is too short for the finite spatial resolution LES to 'degrade' the spectrum to the form it has when periodic boundary conditions are imposed.

The results suggest that the generation of inflow data is efficient and satisfactory, and thus provide confidence in the general technique.

4. Combined Oscillatory Through-Flow and Steady Current

Pure oscillatory flow and combined oscillatory flow with a steady current have attracted researchers' attention for decays [1, 4, 7, 10, 9, 13, 14, 18], most of which are experimental works. It is likely that compared with a constant driving force, a time-varying external driving force makes a dramatic difference to the turbulent flow. In their study of channel flow with a roughened (rippled) wall, for example, Chang & Scotti [4] found that the effect of an oscillation in the imposed pressure gradient was to increase the mean drag noticeably. Nevertheless, so far, statistically unsteady turbulent flows driven by time-varying external forces have received less attention, compared with the statistically steady ones[7].

Before implementing unsteady spatial boundary conditions derived from the output of much larger scale computations, e.g. the UK Met Office's Unified Model (UM), in which the unsteadiness is more random, we simulated a combined oscillatory throughflow and steady current (which can be considered as the simplest output of the UM model and is labelled as "C20SOI") over a group of cube arrays using the method described in Section 3 for generating the inflow data. To our knowledge, no computations (or measurements) on such a flow have been attempted before. In order to further validate the inflow technique for unsteady base flow, the results were compared with those obtained by applying a combined oscillatory and steady pressure gradient with streamwise periodic boundary conditions (which is labelled as "C20SOP"). Note that the validation of the inflow method is the focus of the current paper. An investigation of the mechanism imposing an unsteady pressure gradient was not attempted. That is because the street scale flow is driven by the external large-scale flow.

An assumption was made here that at the inlet the turbulent fluctuations, e.g. u_{rms}, v_{rms} , w_{rms} are in phase with the streamwise velocity,

$$U = U_0\,[1.0 + 0.5\sin(2\pi t/T)], \qquad (9)$$

where U is the phase averaged streamwise velocity; U_0 is the mean streamwise velocity of the current; $T = 322.6h/u*$ is the oscillation period. Note $u*$ is the mean friction velocity, h is the height of cube. The computational domain is as figure 1b.

The unsteady pressure gradient for the case C20SOP using periodic boundary conditions in streamwise direction is written as follows,

$$\frac{dP}{dx} = -\frac{\rho}{D}\{u_*[1.0 + 0.5\sin(2\pi t/T)]\}^2, \qquad (10)$$

where $D = 4h$ is the depth of the domain (see figure 1a); ρ is the density; again $u*$ is the mean friction velocity; the oscillation period is the same as that in equation 9. The mean streamwise velocity is assumed approximately as,

$$U = U_0 [1 + \alpha \sin(2\pi t/T - \varphi_U], \quad (11)$$

where α is a parameter to be obtained by using a fitting method; φ_U is the phase lag of the pressure gradient. The velocities r.m.s u_{rms}, v_{rms} , w_{rms} are assumed in the similar form as equation (11), probably with different phase lags.

Note for both cases the Reynolds number based on cube height and maximum U_0 is approximately 5,000. The resolution is LES8 (8 grids on the cube) for both cases. The maximum number of cycles sampled is 17. To get converged phase averaged data, we also averaged over 5 degrees locally, which should produce less than a five-percent error.

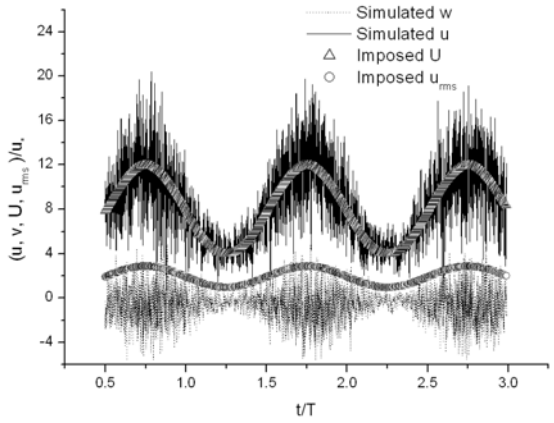

Fig. 6 Times series of simulated streamwise and vertical velocities, and the imposed mean velocity and velocity r.m.s at inlet. T, time period; u_*, friction velocity

Figure 6 is a typical plot which was sampled at the height 2h of C20SOI. It is evident that the simulated velocities are in phase with the imposed U and u_{rms} .

For C20SOI, the phase-averaged statistics were obtained behind row seven at phases ωt = 0, 45, 90, 135, 180, 225, 270, 315(degree) ($\omega t = 2\pi t/T$, see equation 9). For C20SOP, the phase-averaged statistics was obtained at the same eight phases. Then all the phase-averaged statistics on eight phases were algebraically averaged. Figure 7 shows a comparison between C20SOI and C20SOP. There is an evident discrepancy in the upper region in figure 7 (c) and (d), which is surely due to the large length scale, i.e. Lz imposed at the inlet in the vicinity of the upper free-slip wall (see figure 2.). This would be improved by reducing the Lz in the upper part of the flow, as mentioned in the previous section. All the data of C20SOI are also found to be in reasonable agreement with those of the steady base flow in figure 7.

We found that the phase lag φ_U in equation 11 is approximately 30 degree at all heights for C20SOP. Figure 8 shows a comparison of phase averaged streamwise velocity between C20SOI and C20SOP. Note here for C20SOP the phase is $2\pi t/T - \varphi_U$ as in equation 11. Again, for C20SOI the phase-averaged streamwise velocity was obtained behind row seven.

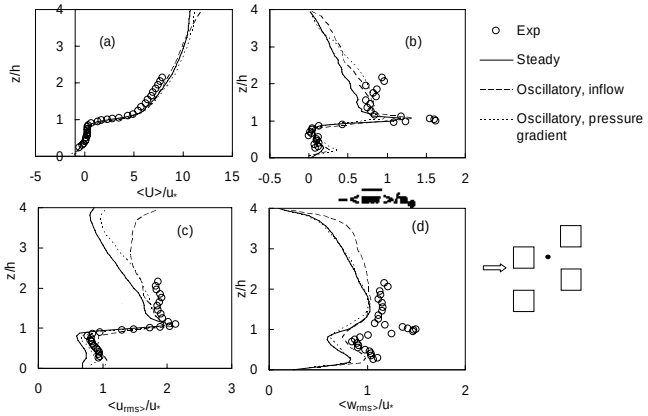

Fig. 7 Algebraically averaged profiles of the phase-averaged statistics

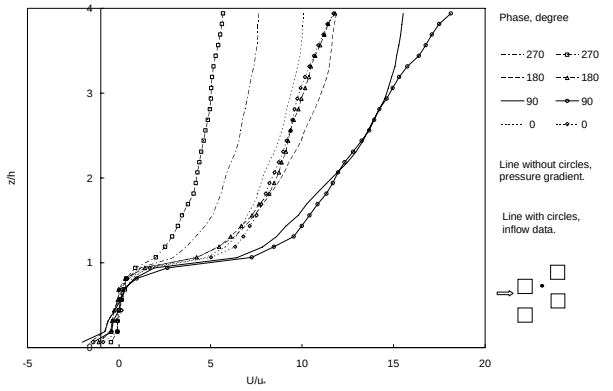

Fig. 8 Vertical profiles of phase averaged streamwise velocity

There is a discrepancy larger than 20 percent on phase 270 degree, at which the streamwise velocity is a minimum. This discrepancy might be caused by the relatively short sampling duration for phase averaging. Turning back to figure 7 (a), note again that the comparison of algebraically averaged profiles of the phase-averaged streamwise velocity is quite satisfactory.

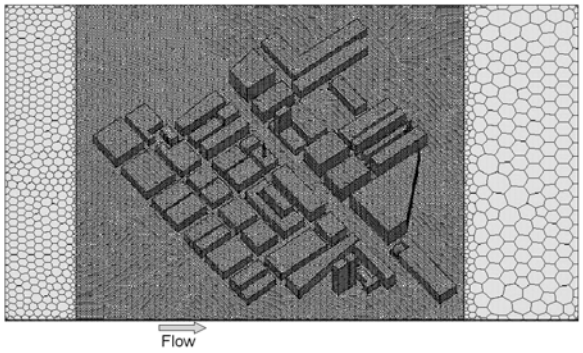

Fig. 9 DAPPLE geometry (a corner of London) and polyhedral mesh

5. Conclusion and Further Work

Firstly, the comparisons between a fully-resolved DNS (64 grids on the cube) computation of flow at $Re=5\times10^3$ over a staggered array of cubes [5] and corresponding LES16 computations are very satisfactory. In particular, if the wall layers are not of interest, the results of LES8 with much coarser mesh are also in reasonable agreement with DNS. Secondly, the new method of generating inflow data is very efficient. It is able to reproduce prescribed second order statistics and correlation functions. The comparison of steady base flow between this method and a periodic boundary condition (imposing steady pressure gradient) is encouraging. Thirdly, we applied the inflow method for simulating combined oscillatory throughflow and steady current over staggered cubes. The simulation was validated by imposing combined oscillatory and steady pressure gradient and setting periodic boundary in the streamwise direction.

We are currently developing tools for implementing spatial boundary conditions derived from the output of much larger-scale computations, like those available from the Met Office's Unified Model, to simulate flows over more complex geometry, e.g. the DAPPLE geometry (see figure 9), where a comprehensive field experiment has been undertaken (http://www.dapple.org.uk/).

Acknowledgment: This project was supported by NCAS, NERC under the Urban Meteorology theme of the Universities Weather Research Network (UWERN, Grant No.DST/26/39). Numerical simulations were performed on the IRIDIS computational system, Information System Services (ISS), University of Southampton and we are grateful for help from ISS staff. The CFD code providers were also very helpful in ensuring appropriate implementations of their codes on the ISS system. We are also grateful to the EnFlo lab, University of Surrey for providing DAPPLE data.

References

[1] Al-Asmi K (1992) Vortex shedding in oscillatory flow, PhD Thesis in Depart. Mech. Eng., University of Surrey.

[2] Britter RE and Hanna SR (2003) Flow and disper- sion in urban areas, *Ann. Rev. Fluid Mech*. **35** 469-496.

[3] Castro IP, Cheng H and Reynolds R (2005) Turbulence over urban-type roughness: deduction from wind tunnel measurements, *Bound. Layer Meteorol*., **118** 109-131.

[4] Chang YS and Scotti A (2004) Modeling unsteady turbulent flows over ripples: Reynolds-averaged Navier-Stokes equation (RANS) versus large-eddy simulation (LES), *J. Geohys. Res*. **109**.

[5] Coceal O, Thomas TG, Castro IP and Belcher SE(2006) Numerical investigation of turbulent flow over cubic roughness arrays, *Bound.-Layer Meterol*., in press.

[6] Collier CG (2005), The impact of urban areas on weather, invited talk, RMetS, Exeter, UK.

[7] Dong YH and Lu XY (2004) Large eddy simulation of a thermally stratified turbulent channel flow with temperature oscillation on the wall, Int. *J. Heat Mass Transfer* **47** 2109-2122.

[8] Hanna SR, Tehranian S, Carissimo B, Macdonald RW & Lohner R. (2002) Comparisons of model simulations with observations of mean flow and turbulence within simple obstacle arrays, *Atmos. Environ*. **36** 5067-5079.

[9] Hino M, Kashiwayanagi M, Nakayama A and Hara T (1983) Experiments on the turbulence statistics and the structure of a reciprocating oscillatory flow, *J. Fluid Mechanics 131* 363-400.

[10] Jensen BL, Sumer BM and Fredsøe J (1989) Turbulent oscillatory boundary layer at high Reynolds numbers, *J. Fluid Mech***. 206**:265-297.

[11] Kanda M, Moriwaki R & Kasamatsu F (2004) Large-eddy simulation of turbulent organized structures within and above explicitly resolved cube arrays. *Bound. Layer Meteorol. 112* 343-368.

[12] Klein M, Sadiki A and Janicka J (2003) A digital filter based generation of inflow data for spatially developing direct numerical simulation or large eddy simulation. *J. Comp. Phys*. **186** 652-665.

[13] Li JC, Zhou JF and Xie ZT (1999) On oscillatory boundary layer, *Advances in Mechanics* **29**(4).

[14] Lodahl CR, Sumer BM and Fredsøe J (1998) Turbulent combined oscillatory flow and current in a pile, *J. Fluid Mech*. **373** 313-348.

[15] Lund T, Wu X and Squires D (1998) Generation of turbulent inflow data for spatially developing boundary layer simulation. *J. Comp. Phys*. **140** 233-258.

[16] Meinders ER & Hanjali´c K(1999) Vortex structure and heat transfer in turbulent flow over a wall-mounted matrix of cubes, *Int. J. Heat Fluid Flow* **20** 255-267.

[17] Mordant N, Metz P, Michel O and Pinton J-F (2001) Measurement of Lagrangian velocity in fully developed turbulence. *Phys. Rev. Lett.* **87**(21).

[18] Sleath JFA (1987) Turbulent oscillatory flow over rough beds, *J. Fluid Mech*.**182** 369-409.

[19] Stoesser T, Mathey F, Frohlich J and Rodi W (2003) LES of flow over multiple cubes. *ERCOFTAC Bulletin No. 56.*

[20] Xie ZT, Castro IP (2006) LES and RANS for Turbulent Flow over Arrays of Wall-Mounted Cubes, submitted to *J. Flow,Turbulence and Combustion.*